

# Nonlinear systems for unconventional computing

Kirill P. Kalinin and Natalia G. Berloff

**Abstract** The search for new computational machines beyond the traditional von Neumann architecture has given rise to a modern area of nonlinear science – development of unconventional computing – requiring the efforts of mathematicians, physicists and engineers. Many analogue physical systems including nonlinear oscillator networks, lasers, and condensates were proposed and realised to address hard computational problems from various areas of social and physical sciences and technology. The analogue systems emulate spin Hamiltonians with continuous or discrete degrees of freedom to which actual optimisation problems can be mapped. Understanding of the underlying physical process by which the system finds the ground state often leads to new classes of system-inspired or quantum-inspired algorithms for hard optimisation. Together physical platforms and related algorithms can be combined to form a hybrid architecture that may one day compete with conventional computing. In this Chapter, we review some of the systems and physically-inspired algorithms that show such promise.

## 1 Introduction

We live in a world dominated by information. Systems that enable faster information processing and decision making are becoming more integrated into our daily lives. This data-intensive science relies on continual improvements in hardware for solving ever growing, e.g. in number of variables and constraints, optimisation problems.

---

Kirill P. Kalinin  
University of Cambridge, Cambridge CB3 0WA, United Kingdom kpk26@cam.ac.uk

Natalia G. Berloff  
Skolkovo Institute of Science and Technology Russian Federation, Bolshoy Boulevard 30, bld. 1  
Moscow, Russia 121205

University of Cambridge, Cambridge CB3 0WA, United Kingdom e-mail: N.G.Berloff@damtp.cam.ac.uk

Digital electronics can no longer satisfy this trend, as exponential hardware scaling (Moore's law) and the von Neumann architecture are reaching their limits [76, 116].

Looking beyond the traditional computing one turns to physical platforms that with their superior speed and reconfigurability and internal parallel processing can provide faster alternatives to solving a specialised class of nonlinear problems. Despite a number of physical systems that were proposed as quantum or analogue simulators and further elucidated in active applied research, significant challenges still remain before scalable analogue processors can be realised and show the superior performance in comparison with the von Neumann computing architecture. Over the years, various unconventional computing techniques were proposed that enable simultaneous communication, computation, and memory access throughout their architecture with the purpose to alleviate the device and system architectural challenges faced by conventional computing platforms.

Neuromorphic computing based on neural networks promises to make processors that use low energies while integrating massive amounts of information. Quantum annealer devices promise to find the global minimum of a combinatorial optimisation problem faster than classical computers. Physical (natural) systems aim to become analogue machines by bridging the physics of a particular system with engineering platforms enhancing performance of machine learning.

A central challenge is in the development of mathematical models – system-inspired computing – linking physical platforms to models of complex analogue information processing. Among such models, those based on principles of neural networks and quantum annealing are perhaps the most widely studied.

A large class of problems that can be solved on physical platforms includes nonlinear programming problems. They seek to minimise some nonlinear objective function  $E(\mathbf{x})$  of real or complex variables in  $\mathbf{x}$  subject to a series of constraints represented by equalities or inequalities, i.e.,  $g(\mathbf{x}) = 0$  and  $h(\mathbf{x}) \leq 0$ . Numerous applications in social sciences and telecommunications, finance and aerospace, biological and chemical industries can be described in this basic framework [94, 8, 82].

Nonlinear optimisation problems are notoriously difficult to solve, and often involve specialised techniques such as genetic algorithms, particle swarm optimisation, simulation and population annealing. Around the vicinity of the optimal solution nonlinear optimisation problems are quadratic to second order, and therefore, Quadratic Programming (QP) for minimising quadratic functions of variables subject to linear constraints is a usual simplification to such problems that can be used with a wide array of applications. QP occurs in various machine learning problems, such as the support vector machine (SVM) training and least squares regression. At the same time, QP and other nonlinear optimisation problems can be mapped to spin Hamiltonians which can be emulated by real physical systems: the degrees of freedom  $\mathbf{x}$  become 'spins,' the cost function  $E(\mathbf{x})$  is a 'Hamiltonian' that specifies the interaction pattern between spins. In this chapter we discuss two possible ways by which the system can find the optimal solution – the ground state of the corresponding spin Hamiltonian – depending on the nature of the system. The system in thermodynamic equilibrium may find the optimal solution by quantum annealing which is executed with the time-dependent Hamiltonian

$$H(t) = \left(1 - \frac{t}{\tau}\right)H_0 + \frac{t}{\tau}H_{\text{objective}}, \quad (1)$$

where  $H_0$  is the initial trivial Hamiltonian whose ground state is known, and  $H_{\text{objective}}$  is the final Hamiltonian at  $t = \tau$  which encodes an original objective function  $E(\mathbf{x})$ . If the system is in thermal equilibrium at all times then it stays close to the ground state, as Hamiltonian parameters are adiabatically varied. A linear time dependence in Eq. (1) is assumed for simplicity but more complex annealing schedules can be used. The time  $\tau$  for obtaining the result of optimisation is much larger than that defined by the inverse of the spectral gap (the distance between the ground state and the lowest excited state) of  $H(t)$  [29]. When spectral gap is large, the coupling to the environment helps the annealer by cooling the system towards its ground state, however, as the system becomes larger and the spectral gap shrinks (typically exponentially fast with the system size) the excited states lead to large errors at the same time slowing down the annealing procedure.

Non-equilibrium systems rely on a different principle of approaching the ground state from below rather than via quantum tunnelling during the adiabatic annealing. The principle of the gain-dissipative simulator is based on a two-stage process: gain increase below the threshold and the coherence of operations at the threshold. Ramping up the gain allows system to overcome its linear losses and to stabilise by the nonlinearity of the gain saturation. The emergent coherent state minimises the losses and, therefore, maximises the total number of particles as it will be explained further below, which leads to minimising a particular functional that can be written as the objective spin Hamiltonian. Close to the threshold, the resulting evolution of the system elements resembles the dynamics of Hopfield networks which were shown to be able to solve quadratic optimisation problems more than thirty years ago [42, 122] by using a system of differential equations that describe the evolution of individual neurons:

$$\frac{dx_i}{dt} = - \sum_{j=1}^N J_{ij} S_j(x_j), \quad (2)$$

where  $x_i$  is an input,  $S_j(x_j)$  is the activation function (e.g. sigmoid), and  $J_{ij}$  is the connectivity matrix among the neurons. Various modifications of Hopfield networks were extensively proposed and studied [2], however, the optimisers based on Hopfield networks were surpassed by other computational methods. This is largely due to the high connectivity between neurons that neural networks require and the concomitant time it takes to evolve large networks on classical hardware. The recent interest in Hopfield networks re-emerged as it became possible to create them in analogue physical systems such as electronic circuits or photonic neural networks. Photonic systems have an advantage over their electronic counterparts due to the picosecond to femtosecond time scale of their operation and as hundreds of high bandwidth signals can flow through a single optical waveguide. This means that a photonic implementation of Hopfield networks as optimisers can have a large dimensionality and dense connectivity as well as a fast convergence time. However, the evolution of Hopfield networks does not necessarily lead to the optimal solution.

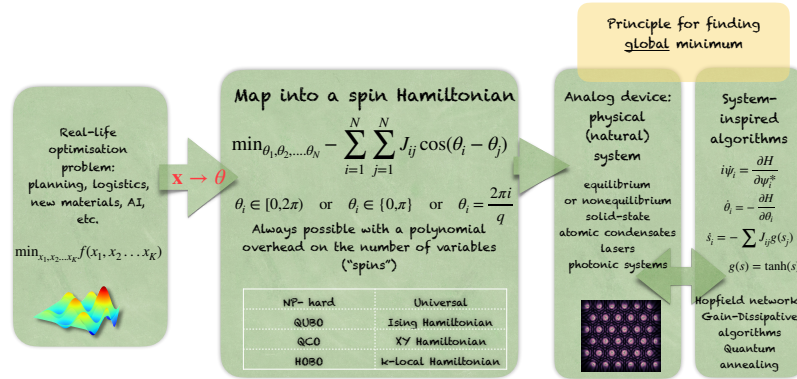


**Fig. 1** Schematics of Hybrid Computing. A computationally hard real life problem can be mapped into a spin Hamiltonian, where spins represent the degrees of freedom (discrete or continuous) of the problem and coupling strengths represent the structure and the constraints of the objective function. Such mapping is possible if the original problem is nondeterministic polynomial, and the resulting spin Hamiltonian is universal. The ground state of the spin Hamiltonian can be found by an analogue physical system using quantum annealing or the gain-dissipative principle of its operation coupled to a digital device (CMOS, FPGA, GPA, etc.) compatible and based on the system-inspired algorithms.

In this Chapter we will review recent progress in building the analogue devices that implement either quantum annealing or gain-dissipative principle in their architecture while illustrating the idea of devising system-inspired algorithms.

## 1.1 Spin Hamiltonians

The majority of optimisation problems are computationally impractical for conventional classical computers with classic examples of a so-called "hard optimisation task" being the travelling salesman problem, the dynamic analysis of financial markets, the prediction of new chemical materials, and machine learning [15]. Mathematically, it is possible to reformulate many of these optimisation problems from vastly different areas as a problem of finding the ground state of a particular spin Hamiltonian with discrete or continuous degrees of freedom, as we will refer to, throughout this Chapter, simply as solving spin model. The spin Hamiltonian can be emulated with a given simulator, e.g. solid-state system, that would need to have an easy mapping of the variables of the desired Hamiltonian into the elements (spins, currents etc.) of the simulator, independently tunable short and long range interactions between them, and would allow one to perform measurements to obtain the answer with the required precision. Such spin model Hamiltonians are experimentally challenging to implement and control but their possible advantageous performance over classical computers, which struggle solving sufficiently large problem sizes, leads to an intensive search for a superior simulator. Such simulators have been proposed

and realised to a various extent in disparate physical systems. Among these systems, two classes of spin Hamiltonians are more common: Ising and XY Hamiltonians. For instance, the Ising Hamiltonian is widely used for a vast variety of hard discrete combinatorial optimisation problems, so that travelling salesman, graph colouring, graph partitioning, and others can be mapped into it with a polynomial overhead [69]. This model is formulated for  $N$  classical “spins”  $s_j$  that take discrete values  $\{-1, 1\}$  to minimise the quadratic unconstrained binary optimisation (QUBO) problem:

$$\min - \sum_{i=1}^N \sum_{j=1, j < i}^N J_{ij} s_i s_j + \sum_{i=1}^N h_i s_i \quad \text{subject to} \quad s_i \in \{-1, 1\} \quad (3)$$

where  $h_i$  represents external (magnetic) field. This term can be incorporated in  $\mathbb{J}$  matrix by considering  $N + 1$  spins and thus will be omitted for the rest of the chapter. Experimental realisation of the nonlinear terms beyond quadratic in the Ising Hamiltonian would lead to a  $k$ -local spin Hamiltonian with  $k > 2$  and would allow for a direct mapping of higher order binary optimisation (HOBQ) problems including Max-SAT [75] or number factorisation [20]:

$$\min - \sum_{i_1, i_2, \dots, i_k}^N Q_{i_1, i_2, \dots, i_k} s_{i_1} s_{i_2} \dots s_{i_l} \dots s_{i_k} \quad \text{subject to} \quad s_{i_l} \in \{-1, 1\}. \quad (4)$$

In the XY model “spins” are continuous  $s_j = \cos \theta_j + i \sin \theta_j$  and the corresponding quadratic continuous optimisation (QCO) problem can be formulated as

$$\min - \sum_{i < j} J_{ij} \mathbf{s}_i \cdot \mathbf{s}_j = \min - \sum_{i < j} J_{ij} \cos(\theta_i - \theta_j) \quad \text{subject to} \quad \theta_i \in [0, 2\pi). \quad (5)$$

When possible phases  $\theta_j$  are limited to discrete values  $2\pi/n$  with an integer  $n > 2$  the model (5) recovers the  $n$ -state Potts model (Clock model) with applications in protein folding [28].

QCO, QUBO, and HOBQ problems are all examples of  $\mathbb{NP}$ -hard problems. The corresponding spin models are universal. The connection between these notions are detailed in the next section.

## 1.2 P, NP, NP-complete problems

The computational complexity of a problem can be revealed by looking at the dependence of the problem’s size on time or the number of operations required to solve it. In a simple case of such polynomial dependence, i.e. when a polynomial time algorithm exists, a problem belongs to a  $\mathbb{P}$  class. If a polynomial time algorithm of finding a solution is not known but there exists a polynomial algorithm for verifying a solution when presented, then a problem belongs to non-deterministic polynomial-

time ( $\text{NP}$ ) class that clearly includes the  $\text{P}$  class. Whether  $\text{P} = \text{NP}$  is true or not is a major unsolved problem in computer science although it is widely believed to be untrue [99]. A problem is  $\text{NP}$ -hard when every problem in  $\text{NP}$  can be reduced in polynomial time to it. The problems that are both  $\text{NP}$ -hard and  $\text{NP}$  are called  $\text{NP}$ -complete. All  $\text{NP}$ -complete problems are equivalent in a sense that either all of them or none of them admit a polynomial-time algorithm. Examples include the travelling salesman problem, spin glass models, and integer linear programming. The computational complexity of finding the ground state of the Ising Hamiltonian (Ising model) on finite lattices has been studied before [10] where the two-dimensional Ising model with a magnetic field (3) and equal antiferromagnetic couplings has been shown to be  $\text{NP}$ -complete for planar graphs. In addition,  $\text{NP}$ -completeness was demonstrated for the three-dimensional Ising model with nearest neighbour interactions and coupling strengths from  $\{-1, 0, 1\}$  [10]. Consequently, the above mentioned hierarchy of complexity classes allows one to conclude the impossibility of existence of a polynomial algorithm for computing the ground state energy of the Ising model without the existence of a polynomial algorithm for all  $\text{NP}$ -complete problems.

The existence of universal spin Hamiltonians has been established. Universality means that all classical spin models with any range of interactions can be reproduced within such a model, and certain simple Hamiltonians such as the 2D Ising model on a square lattice with transverse fields and nearest neighbour interactions are universal [22]. Thus, due to  $\text{NP}$ -hardness of the Ising model, there should exist a polynomial time mapping of many practically relevant  $\text{NP}$ -complete problems to the Ising Hamiltonian, whose decision version solves the  $\text{NP}$ -complete problem of interest. The mapping of various  $\text{NP}$  problems, including Karp's 21  $\text{NP}$ -complete problems [53], to Ising models with a polynomial overhead was demonstrated [69]. For example, the travelling salesman problem for  $N$  cities, that are connected with weighted edges  $w_{uv} \geq 0$  from the set  $E$  (distances between cities), can be formulated as the following Ising problem of size  $N^2$ :

$$\begin{aligned}
 H_{\text{TSP}} = & A \sum_{i=1}^N \left( 1 - \sum_{v=1}^N x_{v,i} \right)^2 + A \sum_{v=1}^N \left( 1 - \sum_{i=1}^N x_{v,i} \right)^2 + A \sum_{(uv) \notin E} \sum_{i=1}^N x_{u,i} x_{v,i+1} \\
 & + B \sum_{(uv) \in E} w_{u,v} \sum_{i=1}^N x_{u,i} x_{v,i+1}.
 \end{aligned} \tag{6}$$

Each spin  $x_{v,i} \in \{0, 1\}$  in Eq. (6) represents the vertex  $v$  and its order  $i$  in a path. All valid routes in this representation are regulated by the first three terms: each city should be in the route (first term) and should appear in it only once (second term), any adjacent cities in the route should be connected (third term), while the search for the optimal route is realised by minimising the sum of weights of all cities in a route (forth term). The reasonable choice of constants  $A$  and  $B$  (e.g.  $A$  should be big enough with respect to  $B > 0$ ) guarantees that only the space of valid routes is explored. Reshaping this two-dimensional spin matrix with elements  $x_{v,i}$  to a spin vector of size  $N^2$  allows one to recover the coupling matrix  $\mathbb{J}$  and magnetic field

$\mathbf{h}$  to formulate the corresponding Ising Hamiltonian. The size of the Ising problem can be reduced to  $(N - 1)^2$  by fixing a particular city to be the first in the route. Note, that the Hamiltonian  $H_{\text{TSP}}$  can represent both directed and undirected graphs, and the generalisation for the cycles optimisation problem is straightforward. We also note that a polynomial overhead does not always apply and some combinatorial optimisation problems can be mapped to the Ising model of the same size  $N$ . For example, the maximum cut (MaxCut) problem

$$\max_{S^+, S^-} \sum_{i \in S^+, j \in S^-} w_{ij} \quad (7)$$

seeks for the cut of a graph into two subsets with a largest sum of their connecting weighted edges. By assigning  $+1$  and  $-1$  spins to all vertices in subsets  $S^+$  and  $S^-$ , respectively, this optimisation problem can be formulated as

$$\max_{s_i} \frac{1}{2} \sum_{i < j} w_{ij} (1 - s_i s_j) = \frac{1}{2} \sum_{i < j} w_{ij} + \min_{s_i} \frac{1}{2} \sum_{i < j} w_{ij} s_i s_j \quad (8)$$

and thus a maximum cut of any graph can be converted to minimisation of the corresponding Ising Hamiltonian with the coupling matrix  $J_{ij} = -w_{ij}$  with an addition of an offset. A well-known standardised set of MaxCut type of problems often serve as a metric for comparison of newly proposed simulators and algorithms [11, 49, 66].

Another example of a universal spin model is the XY model which is directly related to the notoriously hard to solve phase retrieval problem. The problem's objective is to recover a general signal (or image) from the magnitude of its Fourier transform [40, 19, 73]. This problem arises from the fact that the signal detectors can usually record only modulus of the diffraction pattern, therefore, losing the information about the phase of the optical wave. Mathematically, one needs to recover a signal  $\mathbf{x} \in \mathbb{C}^m$  from the amplitude  $\mathbf{b} = |\mathbf{A}\mathbf{x}|$ , where  $A \in \mathbb{C}^{n \times m}$ ,  $\mathbf{b} \in \mathbb{R}^n$ . Then the phase recovery problem [117] can be formulated as:

$$\min_{x_j, u_i} \sum_i \left( \sum_j A_{ij} x_j - b_i u_i \right)^2 \quad (9)$$

where  $\mathbf{u} \in \mathbb{C}^n$  is a phase vector that satisfies  $\mathbf{A}\mathbf{x} = \text{diag}(\mathbf{b})\mathbf{u}$ ,  $|u_i| = 1$  for  $i = \overline{1, n}$ . This optimisation problem can be further rewritten as

$$\min \sum_{ij} M_{ij} u_i u_j \quad \text{subject to} \quad |u_i| = 1, i = \overline{1, n}, \quad (10)$$

where  $M = \text{diag}(\mathbf{b})(I - \mathbf{A}\mathbf{A}^\dagger)\text{diag}(\mathbf{b})$  is the Hermitian matrix,  $I$  is the identity matrix, and  $\mathbf{A}^\dagger$  is the Moore-Penrose pseudoinverse of a matrix  $A$  (see [117] for details).

It is important to note that when we refer to a spin problem as  $\text{NP}$ -complete we understand that for some specific coupling matrix  $\mathbb{J}$  ('problem instances') finding the solution can be easy (belong to  $\mathbb{P}$  class). The term  $\text{NP}$ -completeness reflects worst case behaviour and may allow a polynomial time to solution for most instances on average. This leads to the cornerstone question of how to distinguish hard instances from simple ones. The answer is especially important for the rivalry between classical hardware and unconventional computing machines which have to compete on problems of known complexity. It is believed that the way to create "hard" instances for spin Hamiltonians resides at the intersection of computational complexity and physics, e.g. the hardness of problems can be connected to the existence of a first-order phase transition in a system (see [38] and references therein). If an instance is indeed hard then it would be difficult to solve even for a medium size on a classical computer since the number of operations grows as an exponential function with the matrix size. Thus, the time required to find reliably the ground state energy should highly depend on the coupling matrix structure  $\mathbb{J}$  and the way it was constructed. For instance, finding the global minimum of the XY model for positive definite matrices remains  $\text{NP}$ -hard due to the non-convex constraints but can be effectively approximated using a semidefinite programming (SDP) relaxation with some performance guarantee [30, 125]. Sparsity also plays an important role and for sufficiently sparse matrices fast methods exist [61]. For spin models, the generation of matrix instances  $\mathbb{J}$  with tunable algorithmic hardness and, preferably, with a specifiable ground state, is an ongoing problem studied by many research teams. An elegant way of creating such problems has been recently proposed by a Microsoft research team [38] who suggested to use the Wishart planted ensemble technique. Having a unified set of optimisation problems with a tunable hardness and known solutions would allow for an objective benchmark of quantum simulators on various physical platforms as well as for classical algorithms. Otherwise, announcements of state-of-the-art platforms and methods, which demonstrated their performance on some random and not necessarily hard instances, would continue to happen.

## 2 Physical platforms for large-scale optimisation

Rather than trying to model nature one can consider a reverse idea of exploiting physical phenomena for solving  $\text{NP}$ -complete problems. Such problems can be tackled by quantum computers or simulators to produce solutions in reasonable time. In the last five years we have seen a competition of different physical platforms in solving classical optimisation problems faster than it can be achieved on a classical hardware for a given problem size. This rivalry resulted in the rapid emergence of a new field at the intersection of laser and condensed matter physics, engineering and complexity theories, which aims to develop quantum or classical analogue devices to simulate spin Hamiltonians. Next we discuss the achieved success in such simulations for a range of physical systems.



## 2.1 Cold atoms in optical lattices

Ultracold atoms in optical lattices constitute a well-controlled experimental setting to realise various spin Hamiltonians [45, 14]. Optical lattices are formed by directing several laser beams to interfere and to create standing wave configurations. Such waves provide practically loss-free external potentials in which ultracold atoms may condense, move and interact with one another [34, 123]. The unprecedented control and precision with which one can engineer such lattices and load the atoms there led to many suggestions to consider such systems as possible candidates for unconventional computing in quantum information processing and quantum simulations.

Here we will only discuss a weakly interacting Bose gas in an optical lattice. The description of particles in the strongly-correlated regime is possible with Bose- and Fermi-Hubbard models as well as with extended Hubbard models with nearest-neighbour, next nearest-neighbour interactions, etc. [25]. If the bosonic gas is dilute, the time evolution of the condensate wave function  $\psi$  is governed by the Gross-Pitaevskii equation (GPE) [35, 85, 84]

$$i\hbar \frac{d}{dt} \psi(\mathbf{r}, t) = -\frac{\hbar^2}{2m} \nabla^2 \psi(\mathbf{r}, t) + V_{\text{ext}}(\mathbf{r}) \psi(\mathbf{r}, t) + g |\psi(\mathbf{r}, t)|^2 \psi(\mathbf{r}, t), \quad (11)$$

where  $g$  is the strength of the delta-function interactions and the external potential  $V_{\text{ext}}$  describes an optical lattice – periodic potential – usually combined with a weak harmonic trapping potential.

The condensate evolution and particles' interactions at different local minima of the optical lattice in superfluid regime can be described with the tight-binding approximation, which is valid when the barrier between the neighbouring sites is much higher than the chemical potential. In this approximation the condensate wavefunction  $\psi$  is written as a sum of normalized wave functions  $\phi_i = \phi(\mathbf{r} - \mathbf{r}_i)$  localized in each minimum of the periodic potential, i.e.  $\mathbf{r} = \mathbf{r}_i$ :

$$\psi(\mathbf{r}, t) = \sum_i \Psi_i(t) \phi(\mathbf{r} - \mathbf{r}_i), \quad (12)$$

where  $\Psi_i(t) = \sqrt{\rho_i(t)} e^{i\theta_i(t)}$  is the complex amplitude of the  $i$ -th lattice site,  $\rho_i$  and  $\theta_i$  are the number of particles and the phase in the  $i$ -th site, respectively. The amplitude  $\Psi_i$  describes the state of the so-called 'coherent center' located at  $\mathbf{r}_i$ . By inserting this ansatz into Eq. (11) and integrating the spatial degrees of freedom out one obtains the discrete nonlinear Schrödinger (DNLS) equation (see e.g. [27, 3, 113])

$$i\hbar \frac{\partial \Psi_i}{\partial t} = -J(\Psi_{i+1} + \Psi_{i-1}) + \epsilon_i \Psi_i + U |\Psi_i|^2 \Psi_i, \quad (13)$$

where  $J$  is the nearest-neighbour tunnelling rate,

$$J = - \int d\mathbf{r} \left[ \frac{\hbar^2}{2m} \nabla \phi_i \cdot \nabla \phi_{i+1} + \phi_i V_{\text{ext}} \phi_{i+1} \right], \quad (14)$$

$\epsilon_i$  is the on-site energy given by

$$\epsilon_i = \int d\mathbf{r} \left[ \frac{\hbar^2}{2m} (\nabla \phi_i)^2 + V_{\text{ext}} \phi_i^2 \right], \quad (15)$$

and  $U$  is the nonlinear coefficient given by

$$U = g \int d\mathbf{r} \phi_i^4. \quad (16)$$

Such classical lattice models described by DNLS equations represent the mean-field limit of Bose–Hubbard models [74]. The mean-field limit of the non-standard Bose–Hubbard models includes the interactions beyond the nearest neighbours which leads to a generalised DNLS

$$i\hbar \frac{\partial \Psi_i}{\partial t} = -\frac{1}{2} \sum_{\langle i,j \rangle} J_{ij} \Psi_j + (\epsilon_i + U |\Psi_i|^2) \Psi_i, \quad (17)$$

where  $J_{ij}$  is the coupling strength between the  $i$ -th and  $j$ -th coherent centers. If one loads an equal number of particles in each site of the lattice, the ground state of Eq. (17) realises the minimum of the XY Hamiltonian  $-\sum_{\langle i,j \rangle} J_{ij} \cos(\theta_i - \theta_j)$ . This has been experimentally demonstrated in triangular lattices using the atoms motional degrees of freedom and tunable artificial gauge fields [103, 104].

The quantum annealing protocol can in principle be implemented in such a system by using Eq. (1) with  $H_0 = \sum_{\langle i,j \rangle} \cos(\theta_i - \theta_j)$  and  $H_{\text{objective}} = -\sum_{\langle i,j \rangle} J_{ij} \cos(\theta_i - \theta_j)$ . A similar principle of adiabatic quantum annealing has been realised in the famous D-Wave machine that we discuss below.

## 2.2 D-Wave quantum annealer

D-Wave is a first commercially available quantum annealer that is built on superconducting qubits with programmable couplings and specifically designed to solve QUBO problems (3) [46]. By specifying the interactions  $J_{ij}$  between qubits, a desired QUBO problem is solved [47] via a quantum annealing process as in Eq. (1). Adiabatic (slow) transition in time from an initial state of a specially prepared “easy” Hamiltonian to the objective Ising Hamiltonian guarantees that the system remains in the low energy state, which gives the final energy that corresponds to the optimal solution of the QUBO problem.

Many benchmarks on different QUBO problems were performed on a D-Wave One and D-Wave Two machines without a solid demonstration of quantum speedup of annealer over classical algorithms [101, 23, 126]. A better performance was shown for the last 2000-qubit D-Wave machine released in 2017 on a newly proposed synthetic problem class in which the computational hardness is created through frustrated global interactions. The major limitations of D-wave simulators is that each qubit

can be connected to maximum of six other qubits which is the consequence of creating chips with Chimera structure. The next generation of D-Wave quantum computer is expected to be announced in 2019 with a different architecture which would allow for 15 connections per each node. Together with reverse annealing and virtual graphs features a significant performance improvement could be possibly demonstrated.

### 2.3 Complex laser networks

A new generation of complex lasers such as degenerate cavity lasers, multimode fibre amplifiers, large-aperture VCSEL, random lasers have many advantages in comparison with the relatively simple traditional laser resonators in terms of their computing properties [21]. They have a large number of spatial degrees of freedom, their nonlinear interactions within the gain material can be controlled by adjusting the spatial structures of lasing modes, the spatial coherence of emission can be tuned over a wide range, and the output beams may have arbitrary profiles. These properties allow the complex lasers to be used for reservoir computing [18] or for solving hard computational problems.

In laser networks the coupling can be engineered by mutual light injection from one laser to another. This introduces losses that depend on the relative phases between the lasers. Such dissipative coupling drives the system to a phase locking and therefore to a steady state solution of QCO (5), i.e. to the minimum of the XY Hamiltonian [9, 26, 78]. Degenerate cavity lasers are particularly useful as solvers as all their transverse modes have nearly identical quality factor. This implies that a large number of transverse modes lase simultaneously since they all have similar lasing thresholds [21].

The evolution of the  $N$  single transverse and longitudinal modes class-B lasers can be described by the rate equations [90, 80] on the amplitude  $A_i$ , phase  $\theta_i$ , and gain  $G_i$  of the  $i$ -th laser

$$\frac{dA_i}{dt} = (G_i - \alpha_i) \frac{A_i}{\tau_p} + \sum_j J_{ij} \frac{A_j}{\tau_p} \cos(\theta_i - \theta_j), \quad (18)$$

$$\frac{d\theta_i}{dt} = \Omega_i - \sum_j J_{ij} \frac{A_j}{\tau_p A_i} \sin(\theta_i - \theta_j), \quad (19)$$

$$\frac{dG_i}{dt} = \frac{1}{\tau_c} [P_i - G_i(1 + |A_i|^2)], \quad (20)$$

where  $P_i, \alpha_i, \Omega_i$  represent the pump strength, loss, frequency detuning of laser  $i$ , respectively, whereas  $\tau_p$  and  $\tau_c$  denote the cavity round trip time and the carrier lifetime, respectively. The coupling strengths between  $i$ -th and  $j$ -th lasers are represented by  $J_{ij}$ . If the amplitudes of all lasers are equal, Eq. (19) reduces to the system of coupled phase oscillators

$$\frac{d\theta_i}{dt} = \Omega_i - \frac{1}{\tau_p} \sum_j J_{ij} \sin(\theta_i - \theta_j). \quad (21)$$

Equation (27) is a celebrated Kuramoto model of identical oscillators which is widely used to describe the emergence of coherent behaviour in complex systems [63, 62]. By LaSalle Invariance Principle [56] every trajectory of the Kuramoto model converges to a minimum of the XY Hamiltonian.

It was shown that the probability of finding the global minimum of the XY Hamiltonian agrees between experimental realisations of the laser array and numerical simulations of Eqs. (18-20). However, simulating the Kuramoto model of Eq. (27) on the same matrix of coupling strengths gives a much lower probability of finding the global minimum. The conclusion was made that the amplitude dynamics described by Eq. (18) provides a mechanism to reach the global minimum [80] by pumping from below. This suggested that the cavity lasers can be used as an efficient physical simulator for finding the global minimum of the XY Hamiltonian, and therefore, for solving phase retrieval problems.

A digital degenerate cavity laser has recently been shown to solve phase retrieval problems rapidly [112]. It is an all-optical system that uses nonlinear lasing process to find a solution that best satisfies the constraint on the Fourier magnitudes of the light scattered from an object. To make sure that the solution to the phase retrieval problem is found the compact support aperture is introduced inside the cavity that ensures that different configurations of laser phases compete to find the one with the minimal losses. The system combines the advantages of short round-trip times of the order of 20ns and high parallelism in selecting the winning mode.

## 2.4 Coherent Ising Machine

Network of coupled optical parametric oscillators (OPOs) is an alternative physical system for solving the Ising problem ([72] and references therein). Each OPO is a nonlinear oscillator with two possible phase states above the threshold that can be interpreted as binary spin states  $\{-1, 1\}$  with respect to the reference beam. The OPO is stimulated with pulses of light which are then loaded into a loop of optical fiber. Below threshold, pulses of low intensity have random phase fluctuations. Depending on the enforced pulse interactions, the intensities are continuously modulated so that after multiple runs around the loop the final binary phases are formed for all OPOs at about the same time. Driving the system close to this near-threshold regime, the lowest loss configuration state can be found. This state corresponds to the optimal solution of the Ising Hamiltonian and, therefore, the OPO-based simulator is known as the coherent Ising Machine (CIM).

The currently most successful implementations of CIMs have been realised using a fiber-based degenerate optical parametric oscillators (DOPOs) and a measurement based feedback coupling, in which a matrix-vector multiplication is performed on a field-programmable gate array (FPGA) embedded in the feedback loop. The

computational performance of such scalable optical processor, that is bounded by the electronic feedback, was demonstrated for various large-scale Ising problems [72, 37, 16], while a speedup over classical algorithms is an ongoing study [39, 57]. The ability to implement arbitrary coupling connections between any two spins [72] was apparently the main reason to claim a better scalability of the CIM than the quantum annealer, i.e. D-Wave machine [37].

In a Coherent Ising Machine each Ising spin corresponds to a DOPO that is described by a rate equation for the complex amplitude of the signal field  $a_i$ :

$$\frac{da_i}{dt} = pa_i^* - a_i - |a_i|^2 a_i + \sum_j J_{ij} a_j, \quad (22)$$

where the dynamics is defined by a linear pump term  $p$ , normalised linear and nonlinear losses, and mutual couplings  $J_{ij}$ . To experimentally realise these couplings, a portion of light is extracted from the cavity after each round trip. That light is then homodyned against a reference pulse to produce  $a_i$  that is next supplied to FPGA where a feedback signal is computed for each pulse. Lastly, an optical modulator is applied to convert the signal back to light that can be used for the next round trip. The equations (22) are often reformulated in terms of the in-phase and quadrature components  $a_i = c_i + is_i$  giving the equations in real terms:

$$\frac{dc_i}{dt} = \left( p - 1 - (c_i^2 + s_i^2) \right) c_i + \sum_j J_{ij} c_j \quad (23)$$

$$\frac{ds_i}{dt} = \left( -p - 1 - (c_i^2 + s_i^2) \right) s_i + \sum_j J_{ij} s_j. \quad (24)$$

The computational effectiveness of these equations has been demonstrated [107] by tackling small size Ising type problems of order up to 20. In a part devoted to polariton condensates we will show that for achieving the global minimum the realisation of an individual pump variation  $p_i$  for equalising all signal amplitudes  $|a_i|$  is crucial.

Phase-stability for the whole length of the cavity is required which makes the DOPOs system highly susceptible to external perturbations that can affect performance [37]. Furthermore, the nonlinear DOPO generation process demands powerful laser systems and temperature-controlled nonlinear materials, which result in large and complex optical setups. These issues lead to recent proposals of other physical platforms for implementing a CIM-like machine. A CIM based on opto-electronic oscillators with self-feedback was suggested to be more stable and cheaper based on solving Ising optimisation problems on regular and frustrated graphs with up to 100 spins and similar or better performance compared to the original DOPO-based CIM [17]. An analogue all-optical implementation of a CIM based on a network of injection-locked multicore fiber lasers [7] demonstrated a possibility to solve Ising Hamiltonians for up to thirteen nodes. The dynamics of a network of injection-locked lasers was based on nonlinear coupled photon rate equations and the couplings were

implemented using spatial light modulators (SLMs). The couplings were reported to be dependent on the photon numbers that are not known beforehand, which can be a major obstacle on the way of solving a given Ising Hamiltonian with the proposed photonic CIM. To solve this issue, approaches similar to gain variation [49, 50] may be considered in the future. Another large-scale optical Ising machine based on the use of an SLM was experimentally demonstrated by using the binary phases in separated spatial points of the optical wave front of an amplitude-modulated laser beam and realising configurations with thousands of spins with tunable all-to-all pairwise interactions [83].

## 2.5 Photon and Polariton networks

Microcavity exciton-polaritons, or simply polaritons, are quasi-particles that result from the hybridisation of light confined inside semiconductor microcavities and bound electron hole pairs (excitons). The steady states in these nonequilibrium systems are set by the balance between the pumping intensity, coming from the interconversion rate of the exciton's reservoir into polaritons, and losses, happening due to the leakage of photons. Polaritons are bosons and obey Bose-Einstein statistics. They can form a condensed (coherent) state above a critical density [54]. Thus, polaritons offer a unique playground to explore nonequilibrium condensation and related effects in solids. The advantage for such explorations comes from the polariton's small effective mass that is 4-5 orders of magnitude smaller than the electron's mass. The design and choice of material allows one to control the polariton mass and to realise such solid state nonequilibrium condensates not only at cryogenic temperatures but even at room temperature in organic structures. The weak coupling at high temperatures and high pumping intensities transitions continuously to strong coupling at lower temperatures and lower pumping intensities. In the limit of a small gain, i.e. small losses, solid state condensates resemble equilibrium Bose-Einstein condensates (BECs) and in the regime of high gain, i.e. high losses, they approach the lasers. This transition from the equilibrium BECs to normal lasers was described with a unified approach via polariton condensates [13].

In another system, closely resembling the physics of polariton condensates, macroscopic occupation of the lowest mode for a gas of photons confined in a dye-filled optical microcavity was recently shown [59, 60, 58, 95]. The rapid thermalization of rovibrational modes of the dye molecules by their collisions with the solvent and phonon dressing of the absorption and emission by the dye molecules leads to the thermal equilibrium distribution of photons and concomitant accumulation of low-energy photons. Such systems resemble microlasers [118], but unlike microlasers exhibit a sharp threshold which occurs far below inversion.

To realise the lattices of polariton or photon condensates many techniques have been proposed and realised in experiments. Polariton lattices can be optically engineered by injecting polaritons in specific areas of the sample using a spatial light modulator [121, 71, 110, 111, 12]. A variety of potential landscapes to confine

polariton or photons have also been engineered [96, 4, 24]. The rate equations describing the evolution of gain-dissipative condensates in a lattice were derived from the space and time resolved mean-field equations [50, 52] and take a form of the Stuart-Landau equations

$$\dot{\Psi}_i = -iU|\Psi_i|^2\Psi_i + (\gamma_i - |\Psi_i|^2)\Psi_i + \sum_{j \neq i} C_{ij}\Psi_j, \quad (25)$$

where  $\Psi_i = \sqrt{\rho_i} \exp[i\theta_i]$  is the complex amplitude of the  $i$ -th condensate,  $U$  is the strength of self-interactions between the quasi-particles,  $\gamma_i$  is the effective injection rate (the difference between the pumping of the quasi-particles into the system and linear losses). The coupling strength  $C_{ij} = J_{ij} + iG_{ij}$  is generally a complex number and consists of the Heisenberg coupling  $J_{ij}$  mediated by the injection reservoir and the Josephson part  $G_{ij}$  that comes from exchange interactions between the condensates. The system described by Eq. (25) reaches the fixed point when  $J_{ij} \gg G_{ij}$  and the pumping feedback is introduced in the system [50]. The feedback on the pumping intensity ensures that all the occupations are the same at the fixed point, by adjusting the pumping if the occupation exceeds the set threshold value  $|\Psi_i|^2 = \rho_{\text{th}}$ . The total injection of the particles in the system of  $N$  condensates at the fixed point is given by

$$\sum_{i=1}^N \gamma_i = N\rho_{\text{th}} - \sum_{i=1}^N \sum_{j < i}^N J_{ij} \cos(\theta_i - \theta_j). \quad (26)$$

Choosing the lowest possible total particle injection  $\sum \gamma_i$  that leads to the occupation  $\rho_{\text{th}}$  for each condensate guarantees that the minimum of the XY Hamiltonian is reached. In order to find the true global minimum the system has to slowly be brought to the condensation threshold while spending enough time in its neighbourhood to span various phase configurations driven by the system noise (classical and quantum fluctuations). When the system reaches a phase configuration in the vicinity of the minimum of the XY Hamiltonian it quickly converges to it by the gradient decent given by the imaginary part of Eq. (25):

$$\dot{\theta}_i = -U\rho_{\text{th}} - \sum_{j \neq i}^N J_{ij} \sin(\theta_i - \theta_j). \quad (27)$$

This idea has been theoretically justified [50] and experimentally realised for simple polariton graphs [12]. It was also proposed how to extend the scheme to discrete optimisation problems such as QUBO (minimising the Ising Hamiltonian) or  $n$ -states Potts Hamiltonians [51]. When the resonant excitation is combined with a non-resonant one, the spins are forced to take the discrete values aligning with the directions set by the resonant excitation. If  $n : 1$  resonant drive is added to the system, the dynamics of the coherent centres obeys

$$\dot{\Psi}_i = -iU|\Psi_i|^2\Psi_i + (\gamma_i - |\Psi_i|^2)\Psi_i + \sum_{j \neq i} J_{ij}\Psi_j + h(t)\Psi_i^{*(n-1)}, \quad (28)$$

where  $h(t)$  is an increasing function that reaches some value  $H > \max_i \sum_j |J_{ij}|$  at the threshold density  $\rho_{th}$ . The adjustment of injection rates leads to the equal-density fixed point and Eq. (26) becomes

$$\sum_{i=1}^N \gamma_i = N\rho_{th} - \sum_{i=1}^N \sum_{j<i}^N J_{ij} \cos(\theta_i - \theta_j) - H\rho_{th}^{n/2-1} \cos(n\theta_i). \quad (29)$$

At  $n = 2$ , the last term on the right-hand side provides the penalty to phases deviating from 0 or  $\pi$  reducing the optimisation problem to QUBO. For  $n > 2$ , the  $n$ -state Potts Hamiltonian is minimised. The minimisation of HOBO may be achieved when the system operates much above the threshold and higher order terms can not be neglected [102].

If the time evolution of the reservoir of noncondensed particles is slow, the system of  $N$  interacting coherent centres is better described by the following equations [52]:

$$\dot{\Psi}_i = -iU|\Psi_i|^2\Psi_i + (R_i - \gamma_c)\Psi_i + \sum_{j\neq i} J_{ij}\Psi_j, \quad (30)$$

$$\dot{R}_i = \Gamma_i - \gamma_R R_i - R_i|\Psi_i|^2, \quad (31)$$

where  $R_i$  is the occupation of the  $i$ -th reservoir,  $\Gamma_i$ ,  $\gamma_R$  and  $\gamma_c$  characterize the rate of particle injection into the reservoir and the linear losses of the reservoir and condensate, respectively. If one replaces  $\Psi_i$  by the electric field and  $R_i$  by the population inversion of the  $i$ -th laser, the result is a form of the Lang-Kobayashi equations normally derived to describe the dynamical behavior of coupled lasers from Lamb's semiclassical laser theory [64, 1]. The total injection of the particles in the system of  $N$  condensates at the fixed point is given by

$$\sum_{i=1}^N \Gamma_i = (\gamma_R + \rho_{th})[N\gamma_c - \sum_{i=1}^N \sum_{j<i}^N J_{ij} \cos(\theta_i - \theta_j)]. \quad (32)$$

Similar to Eq. (26), if the total injection into the system is minimal, the phases of coherent centres minimise the XY Hamiltonian.

Next we discuss the current and future role of physical systems mentioned above in a rapidly developed machine learning applications.

### 3 Analogue Physical Systems for Recurrent Neural Networks and Reservoir Computing

The artificial neuron (perceptron) is a weighted decision-making procedure that takes binary input vector and produces a single binary output [91]. For a stable learning process, a small change in a weight (or bias) should cause only a small change in the output so that a few updates of parameters with a technique such as



backpropagation [92] can produce a better output. Such condition doesn't hold for a perceptron network that is sensitive to small changes in parameters of any single neuron. Introducing a nonlinear activation function helps to overcome this problem with common choices for the function being the sigmoid, tanh, and the rectified linear unit. With an addition of intermediate layers of neurons, hidden layers, the architecture and the training of the network can become nontrivial. The final design usually is a trade off between the number of hidden layers against the time required to train the network. In fact, even optimising the design for single hidden-layer networks is an NP-hard problem [15]. The outputs in each layer can be calculated given the outputs from the lower layers, so the information is always transmitted forward.

Such feedforward neural networks are powerful learning models that have shown state-of-the-art results on a variety of machine learning applications [93] though they were still limited to the tasks with independent training and test data points. Addressing the data with time and space relationships (e.g. video frames and audio snippets) requires backward connection between layers of neurons, and so better modelled with recurrent neural networks (RNNs).

The capability of RNNs with nonlinear activations to perform nearly arbitrary computation was demonstrated with a simulation of a universal Turing machine [98]. The two well-known RNN architectures for sequence learning were introduced later: long short-term memory [41] and bidirectional recurrent neural networks [97]. The former introduced the memory cell, a unit of computation that replaces traditional nodes in the hidden layer of a network, while the latter proposed that the output at any point in the sequence should be dependent on information from both the future and the past (comprehensive reviews of RNNs can be found in [124, 68]). Following [68], the input (target) sequence to a simple RNN with one hidden layer can be denoted as a sequence of vectors  $\mathbf{x}^{(t)}$  ( $\mathbf{y}^{(t)}$ ) for  $t = \overline{1, T}$ . The RNN will then produce predicted vectors  $\hat{\mathbf{y}}^{(t)}$  at each time step:

$$\mathbf{h}(t) = f_{\text{activation}}^{(1)} \left( W^{hx} \mathbf{x}(t) + W^{hh} \mathbf{h}(t-1) + \mathbf{b}_h \right) \quad (33)$$

$$\hat{\mathbf{y}}(t) = f_{\text{activation}}^{(2)} \left( W^{yh} \mathbf{h}(t) + \mathbf{b}_y \right) \quad (34)$$

where  $W^{hx}$  ( $W^{yh}$ ) is the weight matrix between the input (output) and the hidden layer,  $W^{hh}$  is the matrix of recurrent weights connecting the hidden layer with itself at adjacent time steps,  $\mathbf{b}_h$  and  $\mathbf{b}_y$  are bias vectors, and  $f_{\text{activation}}^{(i)}$  are nonlinear activation functions. In such RNN, nodes with recurrent edges, i.e. edges that connect adjacent time steps, receive input from both the current state  $\mathbf{x}(t)$  and from the previous state via hidden node values  $\mathbf{h}(t-1)$ . Given the hidden node values  $\mathbf{h}(t)$ , the output values  $\hat{\mathbf{y}}(t)$  are calculated which can be affected by the input  $\mathbf{x}(t-1)$ . Such cyclic network can still be trained across many time steps using backpropagation through time [120] since RNNs can be interpreted as a deep network with one layer per time step and shared weights across time steps.

RNNs constitute a natural approach to numerous problems ranging from handwriting generation [33, 32] to character prediction [105] to machine translation

[48, 106]. Such successful results and computational hardness of learning process make recurrent networks a great candidate for simulations with a physically based platform. Such physical systems can be much more efficient than any of known classical hardware implementations due to the inherent physical properties such as quantum or classical parallelism and neural network-type architecture. A recent mapping of dynamics of acoustic and optical waves to RNNs was suggested [43].

Other computational frameworks for data processing such as reservoir computing (RC) (originally referred to as echo state networks [44] or liquid state machines [70]) can benefit from an implementation with analogue physical platforms. A particular useful property is that RC systems demand lesser precision of individual control of all forward and backward neuron connections. Various nonlinear dynamical systems, including electronic [100, 5, 86], photonic [55, 65], spintronic [109, 77, 89], mechanical [114], and biological [115] systems, have been recently employed as potential reservoirs for RC (see [108] and references therein).

RC methods have been successfully applied to many practical problems involving real data, with focus on machine learning applications. The role of the reservoir (physical system) in RC is to nonlinearly map sequential inputs into a higher-dimensional space so that features can then be extracted from its output with a simple learning algorithm. Therefore, such reservoirs become attractive for an experimental implementation in many physical systems with a motivation of realising fast information processing devices with low learning cost. Networks of polaritons or lattices of atomic condensates, discussed above, can serve as interacting nonlinear elements for an efficient network-type RC system with a possible approach suggested recently [79].

## 4 System-inspired algorithms

The discovered principles of operation of the analogue physical systems for finding optimal solutions lead to the opportunity of formulating new optimisation algorithms to be realised on specialised but classical computing architectures: FPGAs, GPAs, etc.

The principle of operation of the Coherent Ising Machine was implemented as the network of nonlinear oscillators described by simplified equations [67]:

$$\frac{dx_j}{dt} = -\frac{\partial V}{\partial x_j} \quad \text{with} \quad V = \sum_j V_b(x_j) + \epsilon V_H(x_j), \quad (35)$$

where  $x_j$  are  $N$  analogue variables,  $V_b(x_j) = -0.5\alpha x_j^2 + 0.25x_j^4$  is the paradigmatic bistable potential,  $\alpha = -1 + p$  is the bifurcation parameter given by the normalized decay rate and linear gain  $p$  for the signal field,  $\epsilon \ll 1$  is a positive coefficient,  $V_H(x_j) = -\sum_i J_{ij}x_i x_j$  is the analogue of the Hopfield network. The addition of the amplitude variation to these equations [66], i.e.  $\epsilon \rightarrow \epsilon e_j$ , resulted in

$$\frac{de_j}{dt} = \beta(\rho_{\text{th}} - x_j^2)e_j, \quad (36)$$

where  $e_i$  is a positive error variable and  $\beta$  is a positive rate of change of error variables. The initialisation of such additional control of the target amplitude  $\rho_{\text{th}}$  of all analogue variables  $x_j$  allowed to numerically optimise the medium-scale Ising type problems ( $\sim 1000$  spins). A similar approach has been recently realised using FPGAs for a network of Duffing oscillators [31].

Another example of a gain-dissipative algorithm was inspired by the operation of polariton networks [49]. By gradually increasing the pumping strength  $\gamma_i$  for  $i$ -th oscillator while inducing enough noise to span large volume of high dimensional space of the problem one can explore the low energy part of the spin Hamiltonian. This can be achieved by numerical integration of complex fields  $\Psi_i$

$$\dot{\Psi}_i = (\gamma_i - |\Psi_i|^2)\Psi_i + \sum_{j \neq i} J_{ij}\Psi_j + h(t)\Psi_i^{*(n-1)}, \quad (37)$$

$$\dot{\gamma}_i = \epsilon(\rho_{\text{th}} - \rho_i), \quad (38)$$

with the meaning of parameters explained above. The performance of this algorithm was demonstrated on the medium scale Ising and XY models [49].

## 5 Conclusions and Future Challenges

What promise does unconventional computing platform hold? Would it be able to find a better solution in a fixed time? Or find a solution for a fixed precision faster? Or solve more complex problems at fixed and limited cost? Would it appear as an accelerator in neural networks, machine learning and artificial intelligence platforms? Would it be able to solve a full range of different problems or perform a single computationally intensive task or operation as a part of a hybrid platform? The answer "yes" to any of these challenges could imply high technological gains from predicting and developing new materials and designs to creating fully automated AI-controlled systems.

In the short term one may anticipate appearance of a plethora of disparate unconventional computing systems designed to execute specific algorithms or solving a particular practically relevant task. These will be more energy-efficient and will demonstrate a superior performance over classical hardware architectures. These systems could be further orchestrated together to perform larger tasks. The role of orchestra conductor could be devoted to traditional computing resources including CPUs, GPUs, FPGAs, and others. Such symbiosis of classical and unconventional hardware together with the development of system-inspired optimisation algorithms will form an ultimate hybrid computing platform that may allow for continued scaling beyond the physical limits of Moore's law. Many recent proposals exploit this idea, including, for instance, a photonic accelerator for neural networks with weights and inputs encoded in optical signals allowing for the neural network to be repro-

grammed and trained on the fly at high speed [36] and the recurrent Ising machine in a photonic integrated circuit [87].

To characterise the advantages of unconventional computing platforms we can apply the "quantum supremacy" test formulated by John Preskill in 2012 to characterise superior performance of a quantum simulator over any existing classical computing machines [88]. A particular milestone of quantum supremacy has been recently demonstrated with the Google's Sycamore processor [6] based on 53 programmable superconducting qubits for a certain application, namely random circuit sampling. Their claimed speedup of 200s against 10000 years was immediately scaled down to 200s compared to 2 days by using the absolute state-of-the-art classical supercomputer "Summit" at Oak Ridge National Lab [81]. Nevertheless, this is still a remarkable, at least three orders of magnitude acceleration provided by quantum simulations in comparison with classical conventional computing. This achievement is bound to ignite a quantum supremacy race, as already shown by the subsequent boson sampling experiment with tens of photons covering the similar sized Hilbert space as with 48 qubits [119]. In upcoming years, we envision many more systems to actively participate in this race and demonstrate their superior suitability for solving particular classes of problems.

The unconventional computing systems we described in this Chapter are not quantum computers in the traditional meaning of this term. Although quantum effects contribute to the system operation (e.g. Bose-Einstein condensation is a quantum process that obeys quantum statistics), it is not clear if these system offer any quantum speed-up during the search for a solution, e.g. via entanglement and superposition of states. Although, unlike quantum computers these systems have a crucial ingredient that drives their operation: nonlinearity! Nonlinearity leads to the emergence of coherence within each "bit" of the unconventional computers we discussed: a laser, a condensate, an optical parametric oscillator. Nonlinearity drives the gain saturation, mode locking, and coupling.

The physical systems that we described aim at finding the global minimum of hard optimisation problems. All these systems have advantages and limitations. They vary in nonlinearity of the underlying modes of operation, scalability, ability to engineer the required couplings, flexibility of turning the interactions, precision of read-out, factors facilitating the approach the global rather than local minimum. These issues have to be addressed from the experimental point of view in all newly proposed physical platforms.

All of the considered systems in this Chapter have some parts of their operation that promise increased performance over the classical computations. Combined with system-inspired computational algorithms these systems may indeed one day revolutionise our computing.

## 6 Abbreviations

QP      Quadratic Programming

DNLS	Discrete Nonlinear Schrödinger Equation
QUBO	Quadratic Unconstrained Binary Optimisation
QCO	Quadratic Continuous Optimisation
HOBO	Higher Order Binary Optimisation
CIM	Coherent Ising Machine
OPO	Optical Parametric Oscillator
DOPO	Degenerate Optical Parametric Oscillator
FPGA	Field-Programmable Gate Array
SDP	Semidefinite Programming
MaxCut	Maximum Cut
GPE	Gross-Pitaevskii equation
RC	Reservoir Computing
RNN	Recurrent neural networks

## References

1. Juan A Acebrón, Luis L Bonilla, Conrad J Pérez Vicente, Félix Ritort, and Renato Spigler. The kuramoto model: A simple paradigm for synchronization phenomena. *Reviews of modern physics*, 77(1):137, 2005.
2. Sreeram VB Aiyer, Mahesan Niranjan, and Frank Fallside. A theoretical investigation into the performance of the hopfield model. *IEEE transactions on neural networks*, 1(2):204–215, 1990.
3. G. L. Alfimov, P. G. Kevrekidis, V. V. Konotop, and M. Salerno. Wannier functions analysis of the nonlinear schrödinger equation with a periodic potential. *Phys. Rev. E*, 66:046608, Oct 2002.
4. Alberto Amo and Jacqueline Bloch. Exciton-polaritons in lattices: A non-linear photonic simulator. *Comptes Rendus Physique*, 17(8):934–945, 2016.
5. Piotr Antonik. *Application of FPGA to Real-Time Machine Learning: Hardware Reservoir Computers and Software Image Processing*. Springer, 2018.
6. Frank Arute, Kunal Arya, Ryan Babbush, Dave Bacon, Joseph C Bardin, Rami Barends, Rupak Biswas, Sergio Boixo, Fernando GSL Brandao, David A Buell, et al. Quantum supremacy using a programmable superconducting processor. *Nature*, 574(7779):505–510, 2019.
7. Masoud Babaieian, Dan T Nguyen, Veysi Demir, Mehmetcan Akbulut, Pierre-A Blanche, Yushi Kaneda, Saikat Guha, Mark A Neifeld, and N Peyghambarian. A single shot coherent ising machine based on a network of injection-locked multicore fiber lasers. *Nature communications*, 10(1):1–11, 2019.
8. Ryan Babbush, Peter J Love, and Alán Aspuru-Guzik. Adiabatic quantum simulation of quantum chemistry. *Scientific reports*, 4:6603, 2014.
9. Ling Bao, Nam-Heon Kim, Luke J Mawst, Nikolay N Elkin, Vera N Troshchieva, Dmitry V Vysotsky, and Anatolii P Napartovich. Near-diffraction-limited coherent emission from large aperture antiguided vertical-cavity surface-emitting laser arrays. *Applied physics letters*, 84(3):320–322, 2004.
10. Francisco Barahona. On the computational complexity of ising spin glass models. *Journal of Physics A: Mathematical and General*, 15(10):3241, 1982.
11. Una Benlic and Jin-Kao Hao. Breakout local search for the max-cutproblem. *Engineering Applications of Artificial Intelligence*, 26(3):1162–1173, 2013.

12. Natalia G Berloff, Matteo Silva, Kirill Kalinin, Alexis Askitopoulos, Julian D Töpfer, Pasquale Cilibrizzi, Wolfgang Langbein, and Pavlos G Lagoudakis. Realizing the classical xy hamiltonian in polariton simulators. *Nature materials*, 16(11):1120, 2017.
13. NG Berloff and J Keeling. Universality in modelling non-equilibrium pattern formation in polariton condensates. In *Physics of Quantum Fluids*, pages 19–38. Springer, 2013.
14. Immanuel Bloch, Jean Dalibard, and Wilhelm Zwerger. Many-body physics with ultracold gases. *Reviews of modern physics*, 80(3):885, 2008.
15. Avrim Blum and Ronald L Rivest. Training a 3-node neural network is np-complete. In *Advances in neural information processing systems*, pages 494–501, 1989.
16. Fabian Böhm, Takahiro Inagaki, Kensuke Inaba, Toshimori Honjo, Koji Enbutsu, Takeshi Umeki, Ryoichi Kasahara, and Hiroki Takesue. Understanding dynamics of coherent ising machines through simulation of large-scale 2d ising models. *Nature communications*, 9(1):5020, 2018.
17. Fabian Böhm, Guy Verschaffelt, and Guy Van der Sande. A poor man’s coherent ising machine based on opto-electronic feedback systems for solving optimization problems. *Nature communications*, 10(1):1–9, 2019.
18. Daniel Brunner, Miguel C Soriano, Claudio R Mirasso, and Ingo Fischer. Parallel photonic information processing at gigabyte per second data rates using transient states. *Nature communications*, 4:1364, 2013.
19. Oliver Bunk, Ana Diaz, Franz Pfeiffer, Christian David, Bernd Schmitt, Dillip K Satapathy, and J Friso Van Der Veen. Diffractive imaging for periodic samples: retrieving one-dimensional concentration profiles across microfluidic channels. *Acta Crystallographica Section A: Foundations of Crystallography*, 63(4):306–314, 2007.
20. Christopher JC Burges. Factoring as optimization. *Microsoft Research MSR-TR-200*, 2002.
21. Hui Cao, Ronen Chriki, Stefan Bittner, Asher A Friesem, and Nir Davidson. Complex lasers with controllable coherence. *Nature Reviews Physics*, page 1, 2019.
22. Gemma De las Cuevas and Toby S Cubitt. Simple universal models capture all classical spin physics. *Science*, 351(6278):1180–1183, 2016.
23. Vasil S Denchev, Sergio Boixo, Sergei V Isakov, Nan Ding, Ryan Babbush, Vadim Smelyanskiy, John Martinis, and Hartmut Neven. What is the computational value of finite-range tunneling? *Physical Review X*, 6(3):031015, 2016.
24. David Dung, Christian Kurtscheid, Tobias Damm, Julian Schmitt, Frank Vewinger, Martin Weitz, and Jan Klaers. Variable potentials for thermalized light and coupled condensates. *Nature Photonics*, 11(9):565, 2017.
25. Omjyoti Dutta, Mariusz Gajda, Philipp Hauke, Maciej Lewenstein, Dirk-Sören Lühmann, Boris A Malomed, Tomasz Sowiński, and Jakub Zakrzewski. Non-standard hubbard models in optical lattices: a review. *Reports on Progress in Physics*, 78(6):066001, 2015.
26. Vardit Eckhouse, Moti Fridman, Nir Davidson, and Asher A Friesem. Loss enhanced phase locking in coupled oscillators. *Physical review letters*, 100(2):024102, 2008.
27. J Ch Eilbeck, PS Lomdahl, and Alwyn C Scott. The discrete self-trapping equation. *Physica D: Nonlinear Phenomena*, 16(3):318–338, 1985.
28. Magnus Ekeberg, Cecilia Lövkvist, Yueheng Lan, Martin Weigt, and Erik Aurell. Improved contact prediction in proteins: using pseudolikelihoods to infer potts models. *Physical Review E*, 87(1):012707, 2013.
29. Edward Farhi, Jeffrey Goldstone, Sam Gutmann, and Michael Sipser. Quantum computation by adiabatic evolution. *arXiv preprint quant-ph/0001106*, 2000.
30. Michel X Goemans and David P Williamson. Approximation algorithms for max-3-cut and other problems via complex semidefinite programming. *Journal of Computer and System Sciences*, 68(2):442–470, 2004.
31. Hayato Goto, Kosuke Tatsumura, and Alexander R Dixon. Combinatorial optimization by simulating adiabatic bifurcations in nonlinear hamiltonian systems. *Science advances*, 5(4):eaav2372, 2019.
32. Alex Graves. Generating sequences with recurrent neural networks. *arXiv preprint arXiv:1308.0850*, 2013.

33. Alex Graves, Marcus Liwicki, Santiago Fernández, Roman Bertolami, Horst Bunke, and Jürgen Schmidhuber. A novel connectionist system for unconstrained handwriting recognition. *IEEE transactions on pattern analysis and machine intelligence*, 31(5):855–868, 2008.
34. Rudolf Grimm, Matthias Weidemüller, and Yurii B Ovchinnikov. Optical dipole traps for neutral atoms. In *Advances in atomic, molecular, and optical physics*, volume 42, pages 95–170. Elsevier, 2000.
35. Eugene P Gross. Structure of a quantized vortex in boson systems. *Il Nuovo Cimento (1955-1965)*, 20(3):454–477, 1961.
36. Ryan Hamerly, Liane Bernstein, Alexander Sludds, Marin Soljačić, and Dirk Englund. Large-scale optical neural networks based on photoelectric multiplication. *Physical Review X*, 9(2):021032, 2019.
37. Ryan Hamerly, Takahiro Inagaki, Peter L McMahon, Davide Venturelli, Alireza Marandi, Tatsuhiro Onodera, Edwin Ng, Carsten Langrock, Kensuke Inaba, Toshimori Honjo, et al. Experimental investigation of performance differences between coherent ising machines and a quantum annealer. *Science advances*, 5(5):eaau0823, 2019.
38. Firas Hamze, Jack Raymond, Christopher A Pattison, Katja Biswas, and Helmut G Katzgraber. The wishart planted ensemble: A tunably-rugged pairwise ising model with a first-order phase transition. *arXiv preprint arXiv:1906.00275*, 2019.
39. Yoshitaka Haribara, Hitoshi Ishikawa, Shoko Utsunomiya, Kazuyuki Aihara, and Yoshihisa Yamamoto. Performance evaluation of coherent ising machines against classical neural networks. *Quantum Science and Technology*, 2(4):044002, 2017.
40. Robert W Harrison. Phase problem in crystallography. *JOSA a*, 10(5):1046–1055, 1993.
41. Sepp Hochreiter and Jürgen Schmidhuber. Long short-term memory. *Neural computation*, 9(8):1735–1780, 1997.
42. John J Hopfield and David W Tank.  $\tilde{\text{neural}}\tilde{\text{AI}}$  computation of decisions in optimization problems. *Biological cybernetics*, 52(3):141–152, 1985.
43. Tyler W Hughes, Ian AD Williamson, Momchil Minkov, and Shanhui Fan. Wave physics as an analog recurrent neural network. *arXiv preprint arXiv:1904.12831*, 2019.
44. H Jaeger. Technical report gmd report 148. *German National Research Center for Information Technology*, 2001.
45. Dieter Jaksch and Peter Zoller. The cold atom hubbard toolbox. *Annals of physics*, 315(1):52–79, 2005.
46. Mark W Johnson, Mohammad HS Amin, Suzanne Gildert, Trevor Lanting, Firas Hamze, Neil Dickson, R Harris, Andrew J Berkley, Jan Johansson, Paul Bunyk, et al. Quantum annealing with manufactured spins. *Nature*, 473(7346):194, 2011.
47. Tadashi Kadowaki and Hidetoshi Nishimori. Quantum annealing in the transverse ising model. *Physical Review E*, 58(5):5355, 1998.
48. Nal Kalchbrenner and Phil Blunsom. Recurrent continuous translation models. In *Proceedings of the 2013 Conference on Empirical Methods in Natural Language Processing*, pages 1700–1709, 2013.
49. Kirill P Kalinin and Natalia G Berloff. Global optimization of spin hamiltonians with gain-dissipative systems. *Scientific reports*, 8(1):17791, 2018.
50. Kirill P Kalinin and Natalia G Berloff. Networks of non-equilibrium condensates for global optimization. *New Journal of Physics*, 20(11):113023, 2018.
51. Kirill P Kalinin and Natalia G Berloff. Simulating ising and n-state planar potts models and external fields with nonequilibrium condensates. *Physical review letters*, 121(23):235302, 2018.
52. Kirill P Kalinin and Natalia G Berloff. Polaritonic network as a paradigm for dynamics of coupled oscillators. *arXiv preprint arXiv:1902.09142*, 2019.
53. Richard M Karp. Reducibility among combinatorial problems. In *Complexity of computer computations*, pages 85–103. Springer, 1972.
54. Jacek Kasprzak, M Richard, S Kundermann, A Baas, P Jeambrun, JMJ Keeling, FM Marchetti, MH Szymańska, R André, JL Staehli, et al. Bose–einstein condensation of exciton polaritons. *Nature*, 443(7110):409, 2006.

55. Andrew Katumba, Jelle Heyvaert, Bendix Schneider, Sarah Uvin, Joni Dambre, and Peter Bienstman. Low-loss photonic reservoir computing with multimode photonic integrated circuits. *Scientific reports*, 8(1):2653, 2018.
56. Hassan K Khalil. Nonlinear systems. *Upper Saddle River*, 2002.
57. Andrew D King, William Bernoudy, James King, Andrew J Berkley, and Trevor Lanting. Emulating the coherent ising machine with a mean-field algorithm. *arXiv preprint arXiv:1806.08422*, 2018.
58. Jan Klaers, Julian Schmitt, T Damm, F Vewinger, and M Weitz. Bose–einstein condensation of paraxial light. *Applied Physics B*, 105(1):17, 2011.
59. Jan Klaers, Julian Schmitt, Frank Vewinger, and Martin Weitz. Bose–einstein condensation of photons in an optical microcavity. *Nature*, 468(7323):545, 2010.
60. Jan Klaers, Frank Vewinger, and Martin Weitz. Thermalization of a two-dimensional photonic gas in "a white wall" photon box. *Nature Physics*, 6(7):512, 2010.
61. Nathan Krislock, Jérôme Malick, and Frédéric Roupin. Biqcrunch: A semidefinite branch-and-bound method for solving binary quadratic problems. *ACM Transactions on Mathematical Software (TOMS)*, 43(4):32, 2017.
62. Yoshiki Kuramoto. International symposium on mathematical problems in theoretical physics. *Lecture notes in Physics*, 30:420, 1975.
63. Yoshiki Kuramoto. *Chemical oscillations, waves, and turbulence*. Courier Corporation, 2003.
64. Roy Lang and Kohroh Kobayashi. External optical feedback effects on semiconductor injection laser properties. *IEEE journal of Quantum Electronics*, 16(3):347–355, 1980.
65. Laurent Larger, Antonio Baylón-Fuentes, Romain Martinenghi, Vladimir S Udaltsov, Yanne K Chembo, and Maxime Jacquot. High-speed photonic reservoir computing using a time-delay-based architecture: Million words per second classification. *Physical Review X*, 7(1):011015, 2017.
66. Timothée Leleu, Yoshihisa Yamamoto, Peter L McMahon, and Kazuyuki Aihara. Destabilization of local minima in analog spin systems by correction of amplitude heterogeneity. *Physical review letters*, 122(4):040607, 2019.
67. Timothée Leleu, Yoshihisa Yamamoto, Shoko Utsunomiya, and Kazuyuki Aihara. Combinatorial optimization using dynamical phase transitions in driven-dissipative systems. *Physical Review E*, 95(2):022118, 2017.
68. Zachary C Lipton, John Berkowitz, and Charles Elkan. A critical review of recurrent neural networks for sequence learning. *arXiv preprint arXiv:1506.00019*, 2015.
69. Andrew Lucas. Ising formulations of many np problems. *Frontiers in Physics*, 2:5, 2014.
70. Wolfgang Maass, Thomas Natschläger, and Henry Markram. Real-time computing without stable states: A new framework for neural computation based on perturbations. *Neural computation*, 14(11):2531–2560, 2002.
71. Francesco Manni, Konstantinos G Lagoudakis, Timothy Chi Hin Liew, Régis André, and Benoit Deveaud-Plédran. Spontaneous pattern formation in a polariton condensate. *Physical review letters*, 107(10):106401, 2011.
72. Peter L McMahon, Alireza Marandi, Yoshitaka Haribara, Ryan Hamerly, Carsten Langrock, Shuhei Tamate, Takahiro Inagaki, Hiroki Takesue, Shoko Utsunomiya, Kazuyuki Aihara, et al. A fully programmable 100-spin coherent ising machine with all-to-all connections. *Science*, 354(6312):614–617, 2016.
73. Jianwei Miao, Tetsuya Ishikawa, Qun Shen, and Thomas Earnest. Extending x-ray crystallography to allow the imaging of noncrystalline materials, cells, and single protein complexes. *Annu. Rev. Phys. Chem.*, 59:387–410, 2008.
74. RV Mishmash and LD Carr. Ultracold atoms in 1d optical lattices: mean field, quantum field, computation, and soliton formation. *Mathematics and Computers in Simulation*, 80(4):732–740, 2009.
75. Botond Molnár, Ferenc Molnár, Melinda Varga, Zoltán Toroczkai, and Mária Ercsey-Ravasz. A continuous-time maxsat solver with high analog performance. *Nature communications*, 9(1):4864, 2018.
76. Gordon E Moore et al. Cramming more components onto integrated circuits, 1965.



77. Ryosho Nakane, Gouhei Tanaka, and Akira Hirose. Reservoir computing with spin waves excited in a garnet film. *IEEE Access*, 6:4462–4469, 2018.
78. Micha Nixon, Moti Friedman, Eitan Ronen, Asher A Friesem, Nir Davidson, and Ido Kanter. Synchronized cluster formation in coupled laser networks. *Physical review letters*, 106(22):223901, 2011.
79. Andrzej Opala, Sanjib Ghosh, Timothy CH Liew, and Michał Matuszewski. Neuromorphic computing in ginzburg-landau lattice systems. *arXiv preprint arXiv:1808.05135*, 2018.
80. Vishwa Pal, Chene Tradonsky, Ronen Chriki, Asher A Friesem, and Nir Davidson. Observing dissipative topological defects with coupled lasers. *Physical review letters*, 119(1):013902, 2017.
81. Edwin Pednault, John A Gunnels, Giacomo Nannicini, Lior Horesh, and Robert Wisnieff. Leveraging secondary storage to simulate deep 54-qubit sycamore circuits. *arXiv preprint arXiv:1910.09534*, 2019.
82. Alejandro Perdomo-Ortiz, Neil Dickson, Marshall Drew-Brook, Geordie Rose, and Alán Aspuru-Guzik. Finding low-energy conformations of lattice protein models by quantum annealing. *Scientific reports*, 2:571, 2012.
83. D Pierangeli, G Marcucci, and C Conti. Large-scale photonic ising machine by spatial light modulation. *Physical Review Letters*, 122(21):213902, 2019.
84. Lev Pitaevskii and Sandro Stringari. *Bose-Einstein condensation and superfluidity*, volume 164. Oxford University Press, 2016.
85. LP Pitaevskii. Vortex lines in an imperfect bose gas. *Sov. Phys. JETP*, 13(2):451–454, 1961.
86. Anvesh Polepalli, Nicholas Soares, and Dhireesha Kudithipudi. Digital neuromorphic design of a liquid state machine for real-time processing. In *2016 IEEE International Conference on Rebooting Computing (ICRC)*, pages 1–8. IEEE, 2016.
87. Mihika Prabhu, Charles Roques-Carmes, Yichen Shen, Nicholas Harris, Li Jing, Jacques Carolan, Ryan Hamerly, Tom Baehr-Jones, Michael Hochberg, Vladimir Čeperić, et al. A recurrent ising machine in a photonic integrated circuit. *arXiv preprint arXiv:1909.13877*, 2019.
88. John Preskill. Quantum computing and the entanglement frontier. *arXiv preprint arXiv:1203.5813*, 2012.
89. Diana Prychynenko, Matthias Sitte, Kai Litzius, Benjamin Krüger, George Bourianoff, Mathias Kläui, Jairo Sinova, and Karin Everschor-Sitte. Magnetic skyrmion as a nonlinear resistive element: A potential building block for reservoir computing. *Physical Review Applied*, 9(1):014034, 2018.
90. Fabien Rogister, K Scott Thornburg Jr, Larry Fabiny, Michael Möller, and Rajarshi Roy. Power-law spatial correlations in arrays of locally coupled lasers. *Physical review letters*, 92(9):093905, 2004.
91. F Rosenblatt. Principles of neurodynamics (spartan book, washington, dc). 1962.
92. David E Rumelhart, Geoffrey E Hinton, Ronald J Williams, et al. Learning representations by back-propagating errors. *Cognitive modeling*, 5(3):1, 1988.
93. Olga Russakovsky, Jia Deng, Hao Su, Jonathan Krause, Sanjeev Satheesh, Sean Ma, Zhiheng Huang, Andrej Karpathy, Aditya Khosla, Michael Bernstein, et al. Imagenet large scale visual recognition challenge. *International journal of computer vision*, 115(3):211–252, 2015.
94. Giuseppe E Santoro, Roman Martoňák, Erio Tosatti, and Roberto Car. Theory of quantum annealing of an ising spin glass. *Science*, 295(5564):2427–2430, 2002.
95. Julian Schmitt, Tobias Damm, Frank Vewinger, Martin Weitz, and Jan Klaers. Thermalization of a two-dimensional photon gas in a polymeric host matrix. *New Journal of Physics*, 14(7):075019, 2012.
96. Ch Schneider, K Winkler, MD Fraser, M Kamp, Y Yamamoto, EA Ostrovskaya, and Sven Höfling. Exciton-polariton trapping and potential landscape engineering. *Reports on Progress in Physics*, 80(1):016503, 2016.
97. Mike Schuster and Kuldip K Paliwal. Bidirectional recurrent neural networks. *IEEE Transactions on Signal Processing*, 45(11):2673–2681, 1997.
98. Hava T Siegelmann and Eduardo D Sontag. Turing computability with neural nets. *Applied Mathematics Letters*, 4(6):77–80, 1991.

99. Michael Sipser. The history and status of the  $p$  versus  $np$  question. In *Proceedings of the twenty-fourth annual ACM symposium on Theory of computing*, pages 603–618. ACM, 1992.
100. Miguel C Soriano, Silvia Ortín, Lars Keuninckx, Lennert Appeltant, Jan Danckaert, Luis Pesquera, and Guy Van der Sande. Delay-based reservoir computing: noise effects in a combined analog and digital implementation. *IEEE transactions on neural networks and learning systems*, 26(2):388–393, 2014.
101. Damian S Steiger, Bettina Heim, Troels F Rønnow, and Matthias Troyer. Performance of quantum annealing hardware. In *Electro-Optical and Infrared Systems: Technology and Applications XII; and Quantum Information Science and Technology*, volume 9648, page 964816. International Society for Optics and Photonics, 2015.
102. Nikita Stroev and Natalia G Berloff. Discrete polynomial optimization with coherent networks of condensates. *arXiv:1910.00842*, 2019.
103. Julian Struck, Christoph Ölschläger, R Le Targat, Parvis Soltan-Panahi, André Eckardt, Maciej Lewenstein, Patrick Windpassinger, and Klaus Sengstock. Quantum simulation of frustrated classical magnetism in triangular optical lattices. *Science*, 333(6045):996–999, 2011.
104. Julian Struck, Malte Weinberg, Christoph Ölschläger, Patrick Windpassinger, Juliette Simonet, Klaus Sengstock, Robert Höppner, Philipp Hauke, André Eckardt, Maciej Lewenstein, et al. Engineering ising-xy spin-models in a triangular lattice using tunable artificial gauge fields. *Nature Physics*, 9(11):738, 2013.
105. Ilya Sutskever, James Martens, and Geoffrey E Hinton. Generating text with recurrent neural networks. In *Proceedings of the 28th International Conference on Machine Learning (ICML-11)*, pages 1017–1024, 2011.
106. Ilya Sutskever, Oriol Vinyals, and Quoc V Le. Sequence to sequence learning with neural networks. In *Advances in neural information processing systems*, pages 3104–3112, 2014.
107. Kenta Takata, Alireza Marandi, and Yoshihisa Yamamoto. Quantum correlation in degenerate optical parametric oscillators with mutual injections. *Physical Review A*, 92(4):043821, 2015.
108. Gouhei Tanaka, Toshiyuki Yamane, Jean Benoit Héroux, Ryosho Nakane, Naoki Kanazawa, Seiji Takeda, Hidetoshi Numata, Daiju Nakano, and Akira Hirose. Recent advances in physical reservoir computing: a review. *Neural Networks*, 2019.
109. Jacob Torrejon, Mathieu Riou, Flavio Abreu Araujo, Sumito Tsunegi, Guru Khalsa, Damien Querlioz, Paolo Bortolotti, Vincent Cros, Kay Yakushiji, Akio Fukushima, et al. Neuromorphic computing with nanoscale spintronic oscillators. *Nature*, 547(7664):428, 2017.
110. G Tosi, G Christmann, NG Berloff, P Tsotsis, T Gao, Z Hatzopoulos, PG Savvidis, and JJ Baumberg. Sculpting oscillators with light within a nonlinear quantum fluid. *Nature Physics*, 8(3):190, 2012.
111. G Tosi, G Christmann, NG Berloff, P Tsotsis, Tingge Gao, Z Hatzopoulos, PG Savvidis, and JJ Baumberg. Geometrically locked vortex lattices in semiconductor quantum fluids. *Nature communications*, 3:1243, 2012.
112. Chene Tradonsky, Oren Raz, Vishwa Pal, Ronen Chriki, Asher A Friesem, and Nir Davidson. Rapid phase retrieval by lasing. *arXiv preprint arXiv:1805.10967*, 2018.
113. Andrea Trombettoni and Augusto Smerzi. Discrete solitons and breathers with dilute bose-einstein condensates. *Physical Review Letters*, 86(11):2353, 2001.
114. Gabriel Urbain, Jonas Degraeve, Benonie Carette, Joni Dambre, and Francis Wyffels. Morphological properties of mass-spring networks for optimal locomotion learning. *Frontiers in neurobotics*, 11:16, 2017.
115. Philippe Vincent-Lamarre, Guillaume Lajoie, and Jean-Philippe Thivierge. Driving reservoir models with oscillations: a solution to the extreme structural sensitivity of chaotic networks. *Journal of computational neuroscience*, 41(3):305–322, 2016.
116. M Mitchell Waldrop. The chips are down for moore’s law. *Nature News*, 530(7589):144, 2016.
117. Irène Waldspurger, Alexandre d’Áspremont, and Stéphane Mallat. Phase recovery, maxcut and complex semidefinite programming. *Mathematical Programming*, 149(1-2):47–81, 2015.
118. Herbert Walther, Benjamin TH Varcoe, Berthold-Georg Englert, and Thomas Becker. Cavity quantum electrodynamics. *Reports on Progress in Physics*, 69(5):1325, 2006.

119. Hui Wang, Jian Qin, Xing Ding, Ming-Cheng Chen, Si Chen, Xiang You, Yu-Ming He, Xiao Jiang, Z Wang, L You, et al. Boson sampling with 20 input photons in 60-mode interferometers at  $10^{14}$  state spaces. *arXiv preprint arXiv:1910.09930*, 2019.
120. Paul J Werbos et al. Backpropagation through time: what it does and how to do it. *Proceedings of the IEEE*, 78(10):1550–1560, 1990.
121. Esther Wertz, Lydie Ferrier, DD Solnyshkov, Robert Johne, Daniele Sanvitto, Aristide Lemaître, Isabelle Sagnes, Roger Grousson, Alexey V Kavokin, Pascale Senellart, et al. Spontaneous formation and optical manipulation of extended polariton condensates. *Nature physics*, 6(11):860, 2010.
122. GV Wilson and GS Pawley. On the stability of the travelling salesman problem algorithm of hopfield and tank. *Biological Cybernetics*, 58(1):63–70, 1988.
123. Patrick Windpassinger and Klaus Sengstock. Engineering novel optical lattices. *Reports on progress in physics*, 76(8):086401, 2013.
124. Huaguang Zhang, Zhanshan Wang, and Derong Liu. A comprehensive review of stability analysis of continuous-time recurrent neural networks. *IEEE Transactions on Neural Networks and Learning Systems*, 25(7):1229–1262, 2014.
125. Shuzhong Zhang and Yongwei Huang. Complex quadratic optimization and semidefinite programming. *SIAM Journal on Optimization*, 16(3):871–890, 2006.
126. Ilia Zintchenko, Matthew B Hastings, and Matthias Troyer. From local to global ground states in ising spin glasses. *Physical Review B*, 91(2):024201, 2015.

